

The anode erosion phenomenon in a DC non-transferred arc plasma torch

Qiang Sun¹, Yonghong Liu^{1*}, Yejun Zhu¹, Yancong Han¹

¹ China University of Petroleum East China, Qingdao, Shandong, China

Abstract

Anode erosion phenomenon in a DC non-transferred arc plasma torch was experimentally investigated. Anode weight loss and anode erosion position with changes in plasma current, gas-flow rate and anode length were studied. The results show that all these influences could be explained by plasma power. Anode erosion position was closely related to the structure of anode nozzle and the working conditions of plasma torch. The influence of anode arc root position and the energy flow through it on anode erosion was also analyzed. Moreover, the mechanism of anode erosion and its influence on plasma jet were studied. The results can serve as a reference for revealing the mechanism of plasma discharge, for the optimization design of arc plasma torch, and for high-quality plasma generation.

Keywords: anode erosion, non-transferred arc, arc plasma torch, anode arc root

1. Introduction

Direct current non-transferred arc plasma has an irreplaceable role in the synthesis of refractory compounds [1], novel materials [2], nanostructures [3], spray coating [4], and arc-heated thrusters [5-6] due to its extreme energy density, high temperature, steep temperature gradient, and simple control. However, short electrode lifetimes, unreliable torch performance, and lack of flexibility in torch operation inhibit the further industrial application of plasma jets. These factors are direct or indirect consequences of the high erosion rate of electrodes. Extensive research has explored the mechanism and influence factor of electrode erosion, and several applicable measures to decrease electrodes erosion rate have been introduced. Nevertheless, people still have limited knowledge about this phenomenon and the influence of electrode erosion on plasma jets. The erosion of electrodes is closely related to the electron emission current density and the period during which the arc attachment stays in that region. In general, the current density depends on the electrode surface temperature, electric field above the surface, and work function of the surface. I. R. Jankov et al. 7 modified an electrode material by depositing copper on silicon wafer using the electron beam technique and found that this process can yield a work function decrease of 39%; thus, this material can decrease electrode erosion.

Apart from aiming to reduce electron emission current density, extensive research has focused on reducing the period during which the arc attachment stays. An external magnetic field has often been applied to the plasma torch to drive the arc to move rapidly and thereby reduce electrode erosion. R. N. Szenté et al. 8 measured arc velocity driven by a magnetic field B and found that the arc velocity was proportional to $B^{0.60}$ throughout the range investigated. Moreover, erosion rates dropped dramatically with increased arc velocity when an external magnetic field was applied. Similarly, Jin Myung Park et al. 9 developed a 3D transient numerical model to investigate the arc root rotation driven by an external magnetic field and its influence on thermal plasma characteristics in plasma torch. The rotation velocity of the arc root rose in proportion to the square root of the external field strength and increased with the input current but decreased with the gas-flow rate. They confirmed that the application of an external magnetic field is a practical method for driving the rapid rotation of the arc root to diminish electrode erosion.

In another aspect, Pavel Kotalík and Hideya Nishiyama 10 found a recirculation zone in front of the anode of a plasma torch that was consumed faster than other areas. They developed an axisymmetric magneto-

hydrodynamic model for plasma flow in the torch, and the simulation results showed that the application of an external uniform magnetic field parallel to the axisymmetric plasma flow can completely remove or partly decrease the recirculation zone and thereby reduce anode erosion in the near-cathode region.

X. Sun and J. Heberlein [11] investigated the anode erosion phenomenon by a “cold flow” method using a torch having a glass anode with the same geometric dimensions as an actual plasma torch. Density differences between the arc and the cold gas were simulated by injecting heated He from the tip of the cathode into the cold argon gas-flow from a regular gas injector. Micron-sized particles were seeded into the flow to enable the visual observation of the flow trace. The results indicated that a recirculation region existed where the gas-flow met the low-density plasma. This recirculation region overlapped with the erosion area observed in the actual plasma torch.

Renzhong Huangea et al. [12] developed an improved local thermal equilibrium model and applied it to the 3D simulation of the flow patterns inside a plasma torch. They also discussed electric current density and potential. The results showed that the anode erosion was located on the internal surface of the anode, where the largest number of electrons was injected and extended usage only led to an expansion of the erosion range. The results agreed well with the experimental observation.

Several other studies [13-15] showed that the mode of anode attachment (diffused/constricted arc attachment) influences anode erosion rate. Pan Wenxia et al. [16-17] found that diffused arc attachment can only be obtained in pure argon and that the addition of a small amount of nitrogen clearly creates constricted arc root attachment and anode erosion. In their later research [18], a special arc plasma generator was designed, and the sufficiently diffused attachment of the nitrogen arc was realized, thereby reducing the anode erosion rate to a certain extent.

Most existing research has emphasized the approach to reducing electrode erosion. However, in other fundamental areas, few research has focused on the influence factor of anode erosion, erosion position, mechanism of erosion, and influence of anode erosion on plasma jets. In the current work, the relationship between anode erosion and plasma current, anode structure and gas-flow rate were experimentally investigated. A divided anode was used to study the influence of the anode arc root and the energy flow through the arc root on anode erosion. Lastly, the mechanism of anode erosion and its influence on plasma jets was studied. The results can serve as a reference for revealing the mechanism of plasma discharge, for the optimization design of arc plasma jets, and for high-quality plasma generation.

2. Experimental apparatus

Fig. 1 shows the schematic of the experimental apparatus. The plasma spraying torch is homemade, and its dimension is shown in **Fig. 1**. The cathode is water-cooled, and a small cylindrical hafnium is embedded in its tip to reduce the work function. The compression angle of the water-cooled anode is 120° , the bore diameter is 3 mm, and the length of the anode nozzle is L . The distance of the cathode tip to the anode is 2 mm. The anode is designed as a combination to assemble and change it conveniently, and its dimension is shown in **Fig. 1**. Compressed air is used as plasma gas, and gas-flow rate can be regulated by a flow valve and a flowmeter. Two kinds of gas distributors are used, as shown in **Fig. 1**. One can make the gas flow axially and the other make it flow tangentially. In the experiment, the weight loss is measured after a new anode nozzle working for the set time (measurement accuracy: 0.001 g). Every experiment is done three times and the weight loss is got by calculating the average value. A charge-coupled device camera is placed in front of the plasma torch to capture the plasma jet. **Fig. 2** shows the U-I and Power-I property of the homemade plasma power supply (inverter power source, inverter frequency of 20 kHz, constant current source, no-load voltage of 345 V, current adjustment range of 30–200 A, and rated power of 20 kW). The ranges of the working conditions are provided in Table 1.

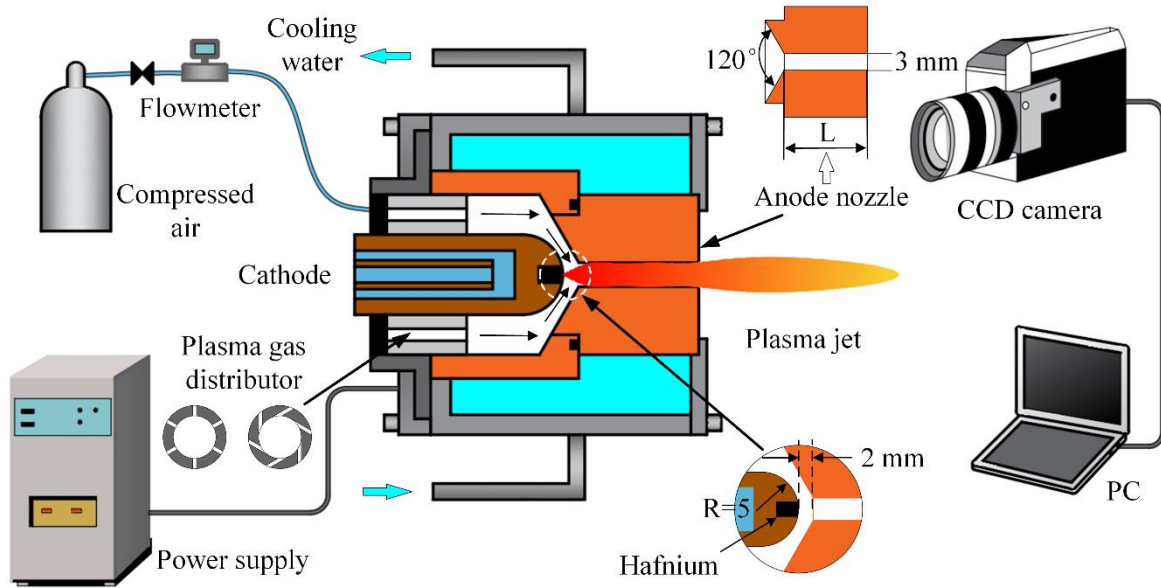


Fig. 1. Schematic of experimental apparatus

Fig. 2(a) shows the U-I property of the plasma power supply. For anode arc root is located in the equilibrium position of gas drag force and electromagnetic force, and there is no inter-electrode insert in the homemade plasma torch, anode arc root moves toward the cathode to make the plasma column short. Besides, larger plasma current can increase ionization extend and reduce impedance of plasma column. These two factors lead to the negative impedance of plasma column and the electrode voltage decreases with the plasma current. Under the same current and anode length condition, the electrode voltage increases with the gas-flow rate because a large gas-flow rate drags the discharge channel longer to increase the electrode voltage. Under the same current and gas-flow rate condition, the electrode voltage decreases with anode length due to the air resistance caused by the anode nozzle. A long anode nozzle can increase air resistance, and the anode arc root moves toward the cathode. This condition shortens the discharge channel and reduces the voltage. **Fig. 2(b)** shows that the plasma power increases with the current. Under the same current and anode length condition, the plasma power increases with the gas-flow rate. Under the same current and gas-flow rate condition, the plasma power decreases with the anode length.

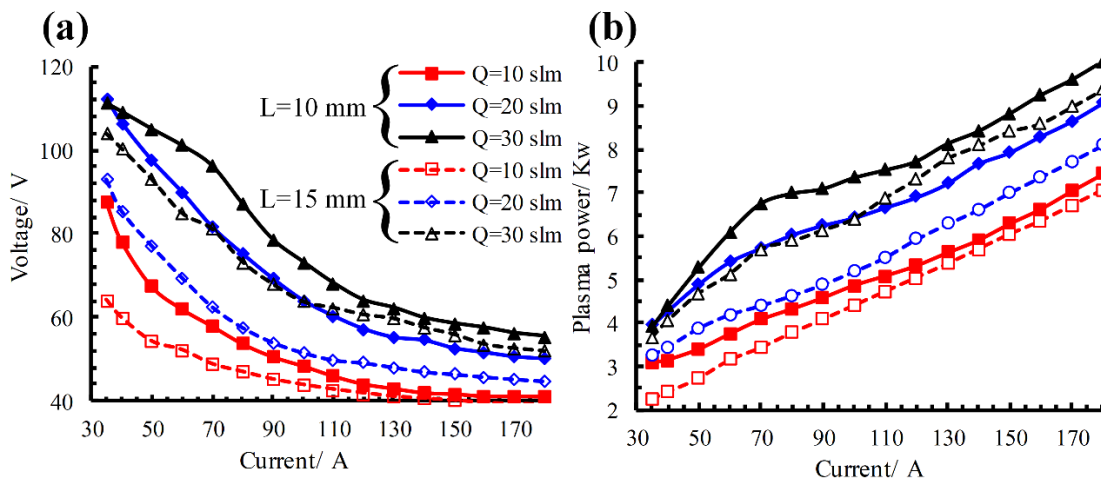


Fig. 2. U-I and Power-I characteristic of homemade plasma power supply

Table 1. Range of working conditions

Bore diameter of anode	3 mm
------------------------	------

Anode nozzle length (L)	10, 15, 20 mm
Arc current (I_p)	40–150 A
Plasma forming gas	Air
Gas-flow rate(Q)	10–40 slm
Anode and cathode material	Copper
Cathode excitation material	Hafnium

3. Results and discussion

3.1 Impact of current on anode erosion

Fig. 3 shows the anode weight loss when the anode length is 10 and 15 mm, respectively, and the gas-flow rate is 20 slm. As shown in **Fig. 3**, anode weight loss increases with changes in working time, and it is closely related to plasma current. Anode weight loss increases with plasma current under the same condition for Joule heat caused by current flow through the anode arc root increases with the plasma current. A large quantity of anode material melts and evaporates with increased current. The dotted lines in **Fig. 3(a)** indicate the weight loss when tangential gas flow is used. There is no significant difference in anode weight loss between the two gas flow conditions and tangential gas flow cannot reduce anode erosion. Moreover, anode weight loss is lower when the anode length is 15 mm than that when the anode length is 10 mm. Hence, a long anode nozzle can reduce anode weight loss (detail analysis can be seen in **3.2** part).

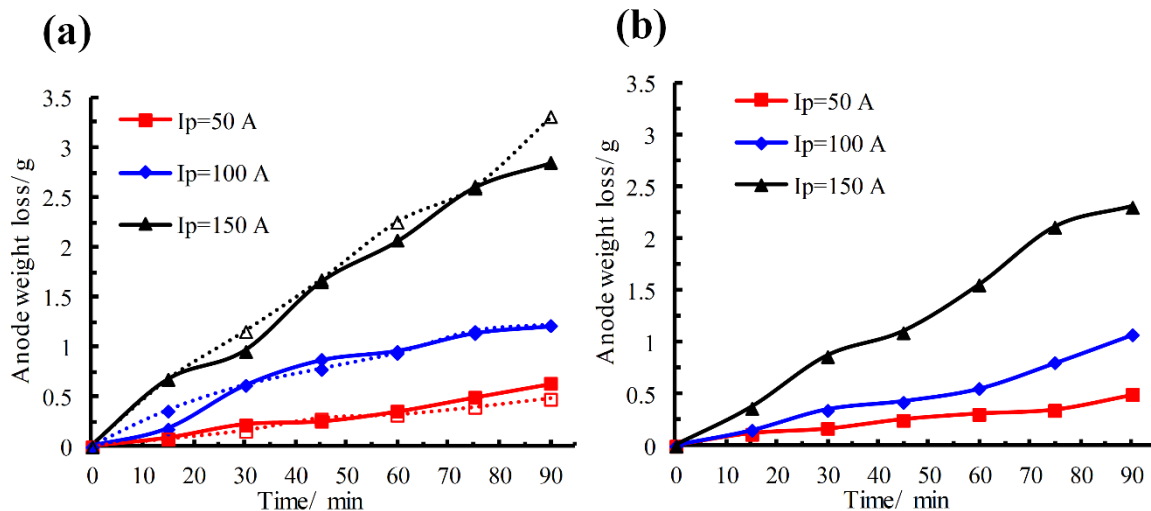


Fig. 3. Anode weight loss with changes in plasma current ($Q = 20$ slm, **(a)** $L = 10$ mm, **(b)** $L = 15$ mm)

Anode weight loss can be used to measure the extent of anode erosion, but it cannot illustrate anode erosion position. The cross section and end view drawings of anodes are observed and researched to review the mechanism of anode erosion.

Fig. 4 shows the cross sections and end view drawings of anodes when the anode length is 10 mm and gas-flow rate is 20 slm. **Fig. 4(a)** shows the anode erosion phenomenon with changes in working time when plasma current is 50 A. The upper part and down part show the axial gas flow manner and tangential gas flow manner, respectively. As shown in **Fig. 4(a)**, the erosion position is near the outlet of the anode nozzle, and the erosion area on the end face increases with working time. The erosion position does not show axial symmetry, and the erosion area is not evenly distributed on the end face. Therefore, the erosion extends along the former erosion area and the eroded area is more likely to be eroded again. A comparison of both axial gas flow manner and tangential gas flow manner shows that tangential gas flow has limited effect in making the erosion distribute evenly.

Fig. 4(b) shows the cross sections and end view drawings of anodes when the working time is 60 min. The

erosion area increases with the plasma current, and the erosion position becomes biased to one side. Especially when the plasma current is 150 A, as shown in **Fig. 4(b)**, the erosion position extends to the edge of anode on one side, whereas no erosion occurs on the opposite side, and the nozzle bore outline can be seen clearly. Thus, the discharge position is more likely to occur in the eroded area, and larger plasma current will intensify this trend.

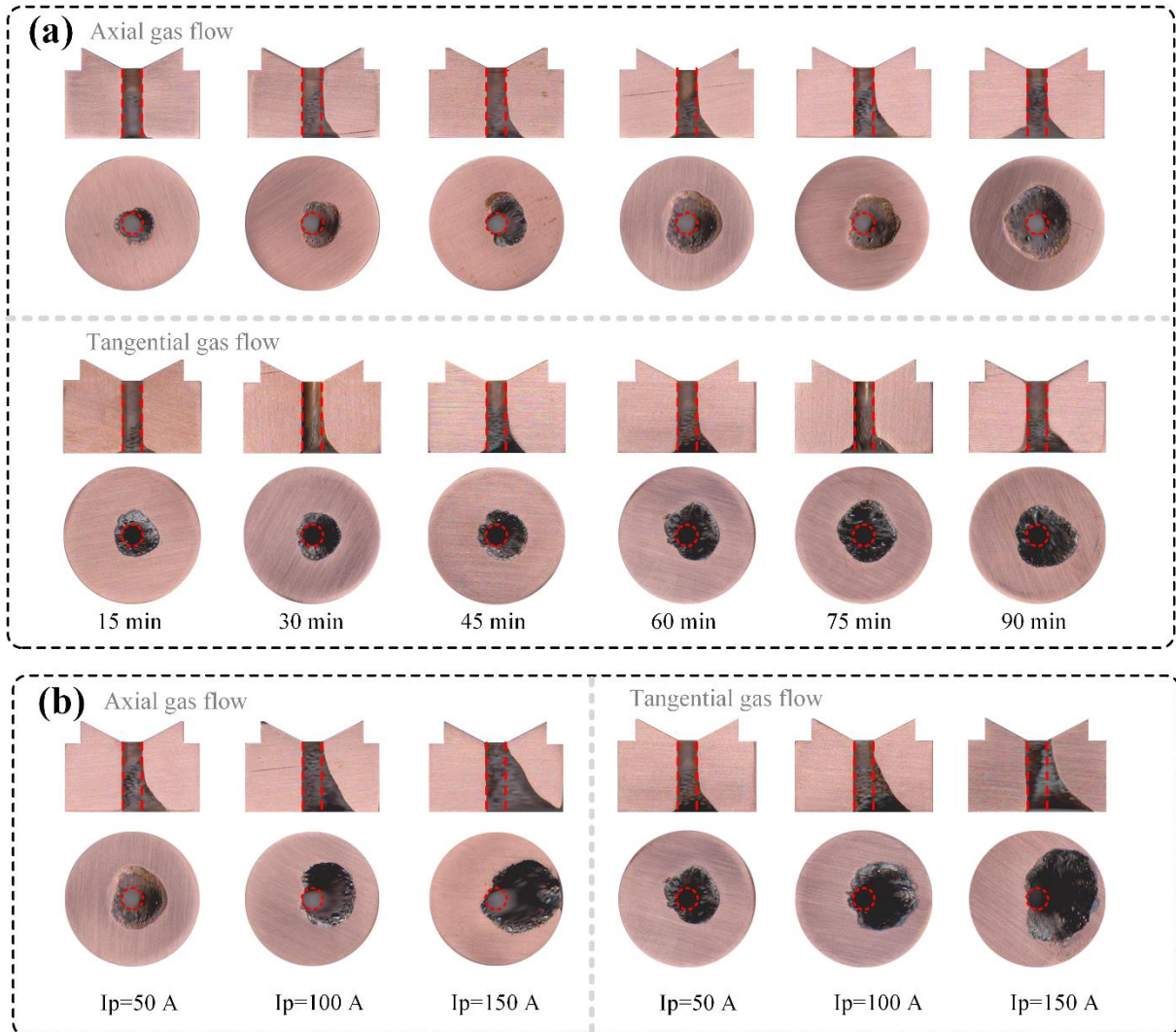


Fig.4 Cross sections and end view drawings of eroded anode ($L = 10$ mm, $Q = 20$ slm (a) $I_p = 50$ A; (b) working time: 60 min)

3.2 Impact of anode length on anode erosion

Fig. 5 shows the anode weight loss when the plasma current is 150 A and the gas-flow rate is 20 slm. Under the same current and gas-flow rate condition, the anode weight loss decreases with the anode length; this result is consistent with the finding in **Figs. 3(a)–(b)**. When the anode nozzle is long, the back and forth movement of the anode arc root covers a great distance. Hence, Joule heat is dispersed on the anode, and material erosion caused by energy concentration is reduced. Moreover, the contact area between the cooling water and the anode increases with the anode length, which in turn increases the cooling effect to reduce anode erosion. Besides, anode length is related to electrode voltage, and the latter determines plasma power. As shown in **Fig. 2**, Plasma power decreases with anode length, and anode weight loss decreases consequently. This is the most important factor.

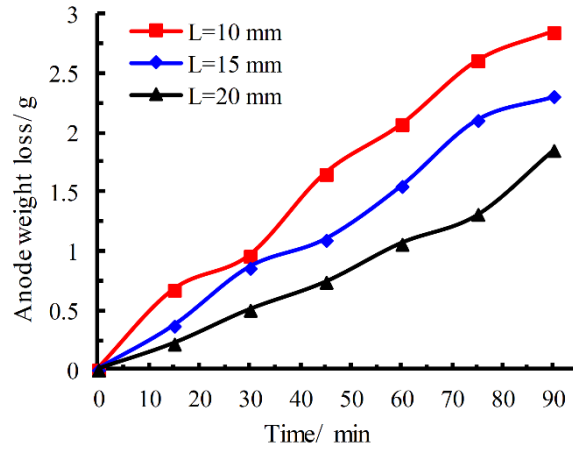


Fig. 5. Anode weight loss with changes in anode length ($I_p = 150$ A, $Q = 20$ slm)

Fig. 6 shows the cross sections and end view drawings of the anodes when the plasma current is 150 A, gas-flow rate is 20 slm, and working time is 60 min. With the increase in anode length, the anode erosion position moves from the outlet of the anode to the inlet. When the anode length is 20 mm, minimal erosion occurs in the outlet, which is completely opposite to the situation when the anode length is 10 mm. Erosion position is related to the position of the anode arc root, and the differential pressure between the cathode chamber and the atmosphere is measured under different anode lengths to illustrate the relationship between anode arc root position and anode length. The results are shown in **Fig. 7**.

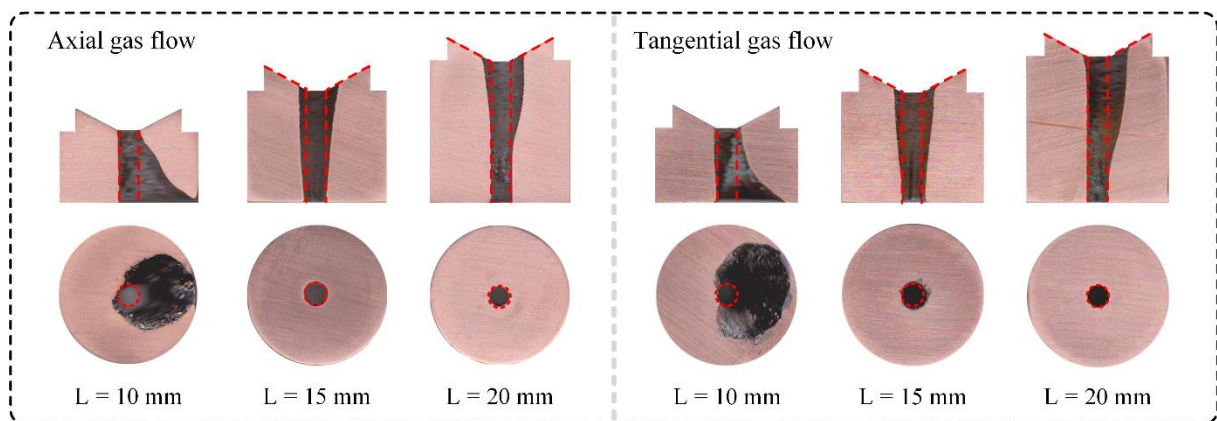


Fig.6 Cross sections and end view drawings of eroded anode ($I_p=150$ A, $Q=20$ slm, $T=60$ min)

Fig. 7 shows the pressure of cathode chamber with changes in plasma current when anode length is 10, 15 and 20 mm, respectively, and gas-flow rate is 20 slm. As shown in **Fig. 7**, the pressure increases with plasma current under the same anode length condition because the heating effect increases and the temperature of the plasma column rises with the increase in current. High temperature will increase the pressure in the plasma column, and the latter causes the rise of cathode chamber pressure. Under the same current, cathode chamber pressure increases with anode length. The viscous resistance of gas increases with the anode length, and the cathode chamber pressure increases.

The position of the anode arc root is determined by the equilibrium position of air drag force and electromagnetic force. When the anode nozzle is short, the air resistance of the anode nozzle is low, and the anode arc root is dragged to the outlet of the anode, making this area the most eroded. When the anode nozzle is long, the air resistance of the anode nozzle is high, and the drag force is abated. As a result, the anode arc root moves toward the cathode, and the inlet area is eroded the most.

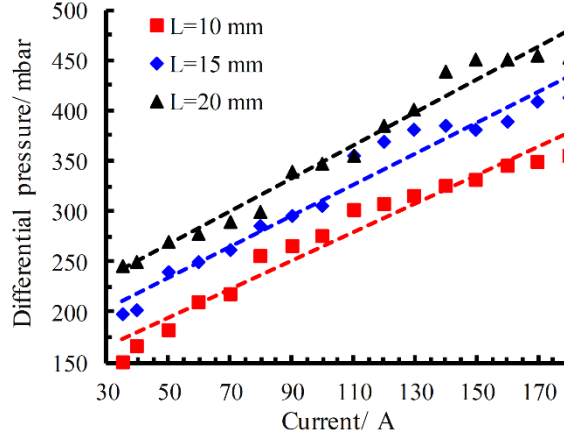


Fig. 7. Pressure of cathode chamber with changes in plasma current (gas-flow rate of 20 slm)

3.3 Impact of gas-flow rate on anode erosion

Fig. 8 shows the anode weight loss when the anode length is 10 and 15 mm, respectively, and plasma current is 100 A. The upper limit of gas-flow rate is 25 and 35 slm, respectively, for the two kinds of anodes. For higher gas-flow rate will make the plasma jet unstable. As shown in Fig. 8(a), anode weight loss increases gradually with changes in gas-flow rate, and when gas-flow rate increases from 15 slm to 20 slm, there is a jump in anode weight loss. After that, anode weight loss stays stable with changes in gas-flow rate. When anode length is 15 mm, as shown in Fig. 8(b), anode weight loss increases slowly first with changes in gas-flow rate ($Q \leq 20$ slm). While gas-flow rate increases to 25 slm, there is a sharp increase in anode weight loss and when gas-flow rate is bigger than 25 slm, anode weight loss will not increase any more.

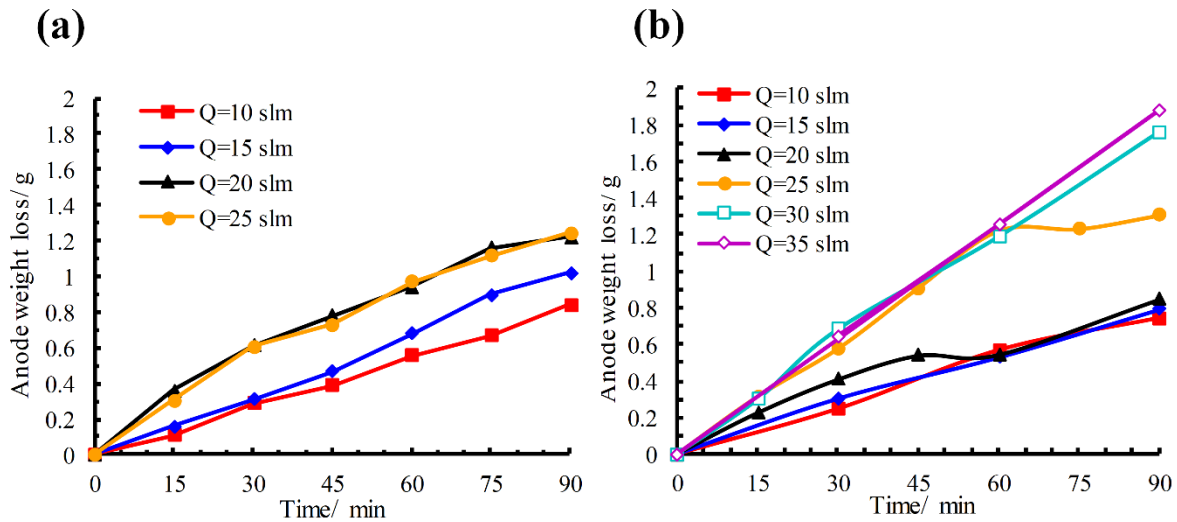


Fig. 8. Anode weight loss with changes in gas-flow rate ($I_p = 100A$, $T=60$ min) (a) $L=10$ mm, (b) $L=15$ mm)

Fig. 9 shows the energy flow through anode with changes in working time. The working condition is the same as that in Fig. 8. The energy is calculated by integrating plasma current multiplied by voltage and time. The current and voltage signals are detected by current sensor and voltage sensor, respectively. The data sampling frequency is 5K. When anode length is 10 mm, as shown in Fig. 9(a), the energy flow through anode increases gradually with gas-flow rate. When gas-flow rate increases to 20 slm, there is a jump in energy and with the continue increase of gas-flow rate, the energy will not increase any more. When anode length is 15 slm, as shown in Fig. 9(b), the tendency is similar with that in Fig. 9(a), but the “jumping value” of gas-flow rate is 25 slm. A comparison of Figs. 8-9 shows that the tendency of anode weight loss is similar with the energy with changes in gas-flow rate. This means anode weight loss is closely related to plasma

power.

With the increase of gas-flow rate, the plasma column can be stretched, and arc voltage can be increased, so the increase of gas-flow rate can increase plasma power under the same current. Higher plasma power causes more anode weight loss. However, with the continuous increase of gas-flow rate, the increasement of plasma power is limited and the thickness of the cold air layer between the arc column and the anode nozzle increases. As a result, the cooling effect of the anode increases. In summary, anode weight loss will not increase any more in high gas-flow rate. The above analysis can illustrate the influence of gas-flow rate on anode erosion, but it cannot explain the jump in anode weight loss with changes in gas-flow rate. In order to further research this phenomenon, the cross sections and end view drawings of the anodes under different gas-flow rate are studied, and the results are shown in **Fig. 10**.

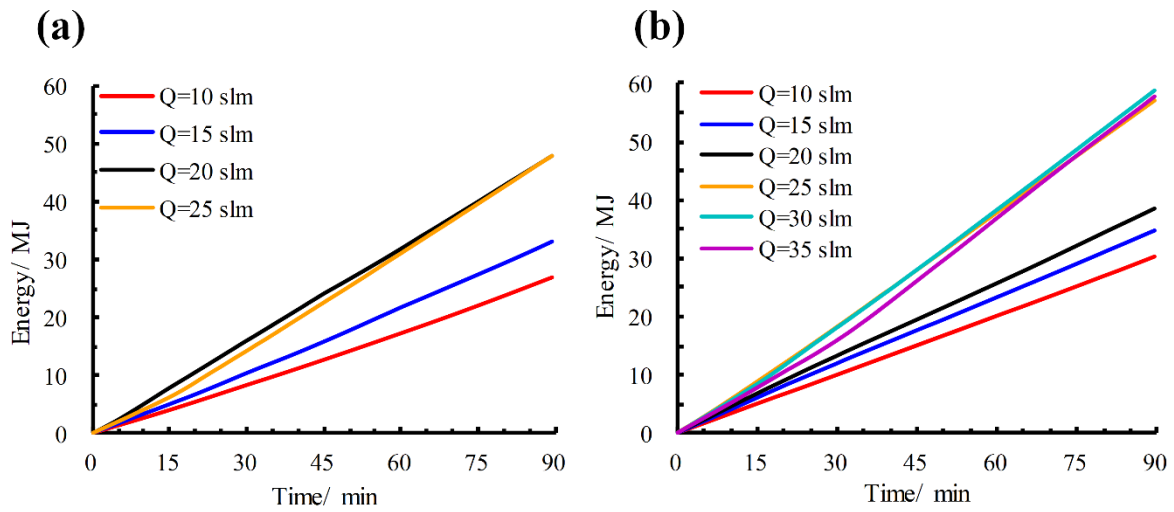


Fig. 9 Energy flow through anode with changes in gas-flow rate ($I_p = 100$ A, (a) $L=10$ mm, (b) $L=15$ mm)

The working condition in **Fig. 10** is the same as that in **Fig. 8** and the working time is 60 min. As shown in **Fig. 10(a)**, the inlet area is eroded when gas-flow rate is lower than 15 slm. When gas-flow rate is higher than 20 slm, the erosion area moves to the outlet of anode. **Fig. 10(b)** shows a similar phenomenon. With the increase of gas-flow rate, the erosion area moves from inlet to outlet of anode, and the threshold value is 25 slm.

A comparison of **Figs. 8-10** shows that the energy flow through anode increases with gas-flow rate, and as a result, the anode weight loss increases. The erosion area moves from inlet to outlet of anode in this process. When anode arc root moves to the outlet of anode, there will be a jump in plasma power and anode weight loss. After that, with the continue increase of gas-flow rate, plasma power and anode erosion will not increase obviously anymore.

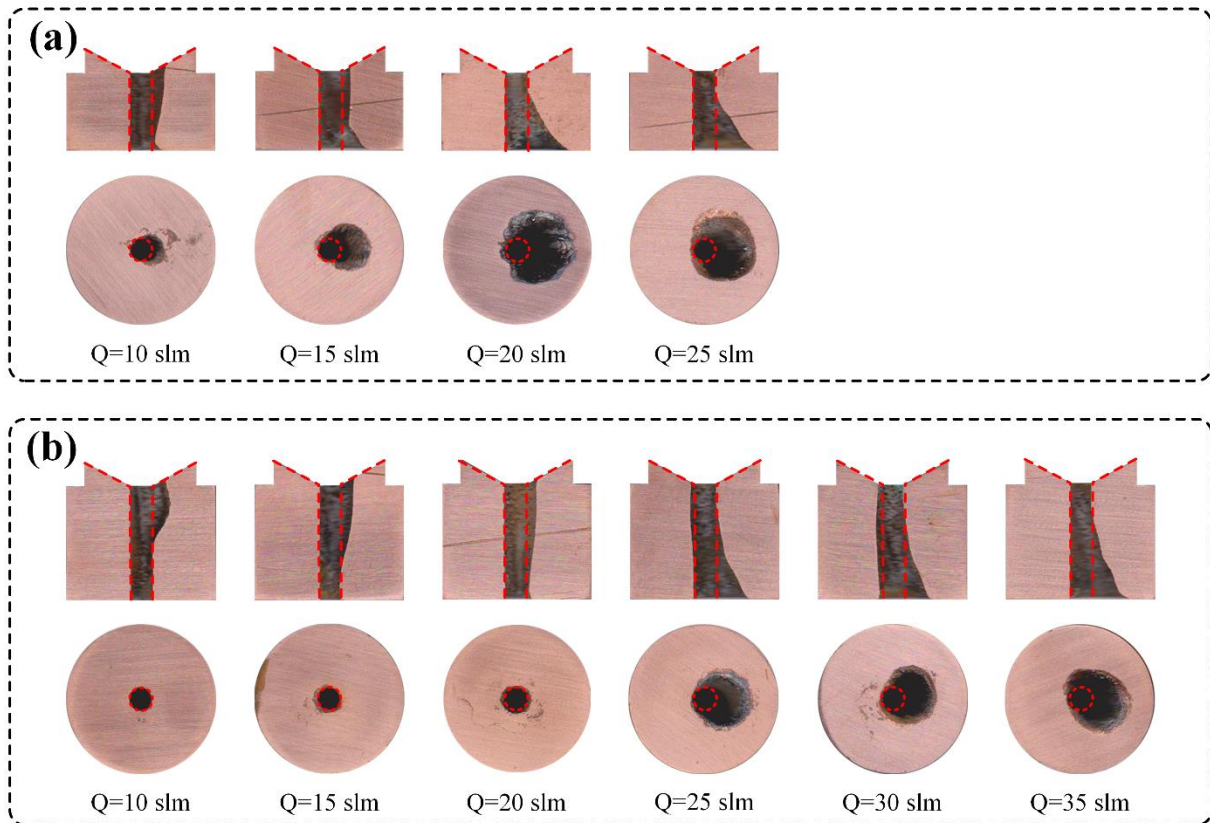


Fig. 10. Cross sections and end view drawings of eroded anode ($I_p = 100A$, (a) $L=10$ mm, (b) $L=15$ mm)

3.4 The mechanism of anode erosion

The above experiments show that anode weight loss is related to the energy flow through anode and the erosion area is related to the position of anode arc root. In order to further illustrate the relationship between anode erosion and the energy flow through the erosion area, divided anodes are used to measure the energy flow through different parts of anode [19]. The schematic of the experiment is shown in **Fig. 11(a)** and **(b)**. The anode is divided into several parts, and a ceramic disc is placed between two adjacent parts. Each part is connected to the positive pole by separated lines. Current sensors and voltage sensor are used to detect the current of each branch and the electrode voltage, respectively (data sampling frequency is 5K). The integral of the current multiplied by voltage and time is the energy flow through the part. **Fig. 11(a)** shows the schematic of the divided anodes when the anode length is 10 mm. The anode is divided into two parts, namely, A and B, starting from the inlet to the outlet, and the thickness of each part is 4.5 mm. The anode length in **Fig. 11(b)** is 15 mm and it is divided into three parts, namely, A, B, and C.

Figs. 11(c)–(d) show the energy flow through each part and the total energy detected by the anode in **Fig. 11(a)** when the plasma current is 50 and 100 A, respectively. **Fig. 11(c)** shows that the discharge mainly occurs in the B section and that the energy proportion of the two parts remains almost constant all the time. This result agrees with the eroded horn-shaped anode (see **Fig. 4(b)**). The result when the plasma current is 100 A is shown in **Fig. 11(d)**. Most discharge occurs in the B section before 75 min, and the energy flow through the A section is low. However, after 75 min, the energy flow through the A section increases because the B section is eroded severely and the eroded area extends to its outer edge. The entire anode becomes horn shaped, and the anode arc root moves to the A section.

Figs. 11(e)–(f) show the energy flow through each part and the total energy detected by the anode in **Fig. 11(b)** when the plasma current is 50 and 100 A, respectively. **Fig. 11(e)** shows that most discharge positions are located in the A and B sections and that the energy of the A section is slightly greater than that

of the B section. This result agrees with the phenomenon when an entire anode (15 mm in length) is eroded such that most areas in the inlet of the anode are eroded severely while the outlet is eroded slightly. **Fig. 11(f)** shows the result when the plasma current is 100 A. Discharge mainly occurs in the A section, and the energy flow through the B section is only approximately 1/2–1/3 of that in the A section because the anode arc root moves toward the cathode with the increase of the plasma current. The anode cross section when the plasma current is 100 A also shows that the inlet of the anode is severely eroded and that the bore is cone shaped (see **Fig. 10(b)**, T=60 min).

The experiment above shows that the divided anode method can be used to predict the anode shape after being eroded. Anode erosion position is related to the position of the anode arc root, and heavy erosion occurs with the increase of the energy flow through the arc root.

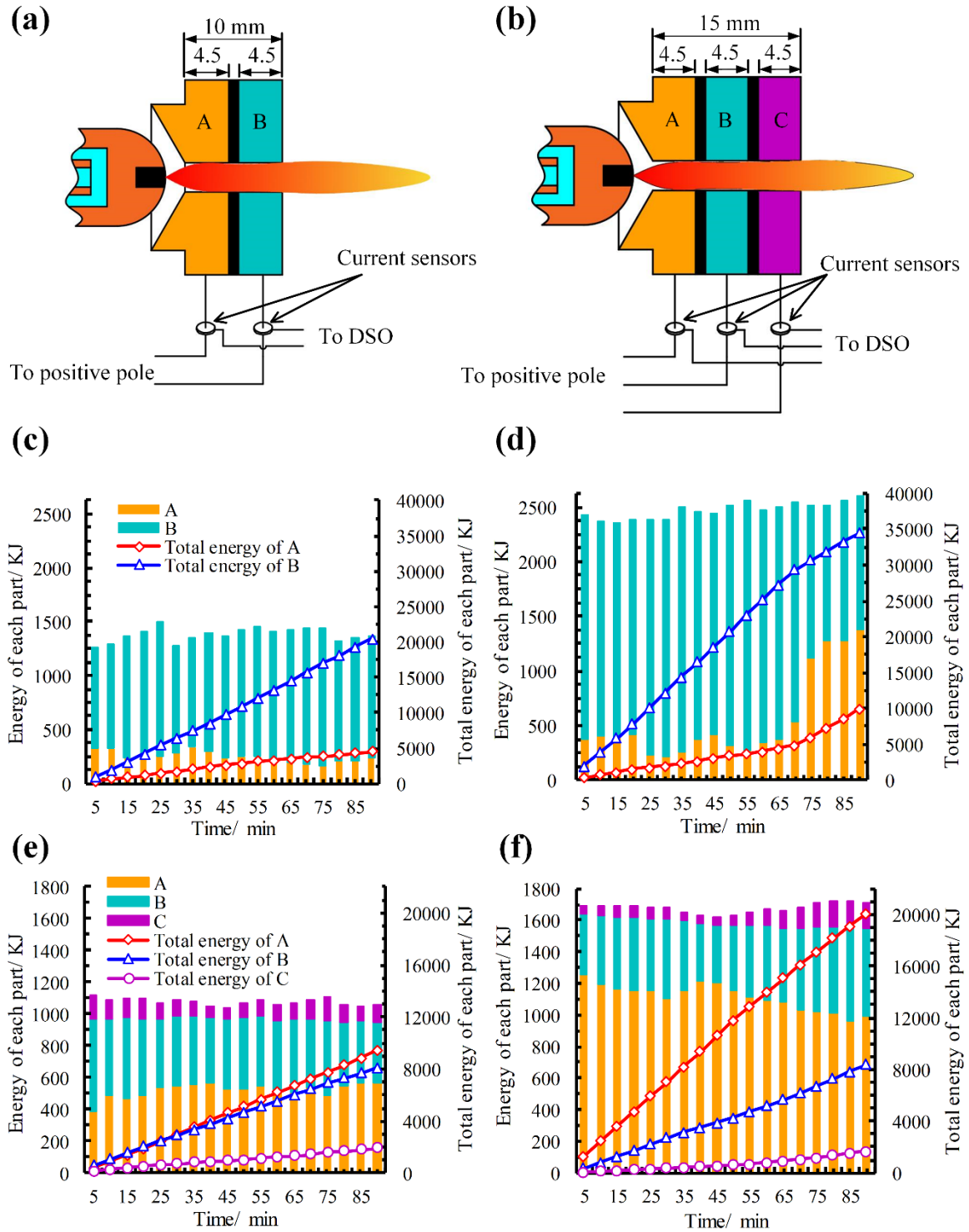


Fig. 11. Schematic of divided anode method and the results((a) $L=10$ mm (b) $L=15$ mm (c) $L=10$ mm, $I_p=50$ A, $Q=20$ slm; (d) $L=10$ mm, $I_p=100$ A, $Q=20$ slm; (e) $L=15$ mm, $I_p=50$ A, $Q=20$ slm (f) $L=15$ mm, $I_p=100$ A, $Q=20$ slm)

Anode erosion is located in the area where the anode arc root occurs, and the question is whether some area can also be eroded while no arc root occurs on its surface. **Fig. 12(a)** shows the schematic of a divided anode with a total length of 15 mm. This anode is divided into two parts by a ceramic disc. The length of the upstream part (A section) is 9 mm, whereas that of the downstream part (B section) is 5 mm. The upstream part remains open while the downstream part is connected to the positive pole of the power supply. In this

situation, the plasma channel passes through a bore measuring 9 mm in length, and no discharge occurs in this section. The anode arc root is dragged to the downstream part. In the experiment, the plasma current is 100 A, the gas-flow rate is 20 slm, and the working time is 60 min. **Fig. 12(b)** shows the cross section of the eroded anode. The anode arc root only occurs in the B section, but erosion is observed on the surface of the A section under the influence of the rapid and hot plasma discharge channel. This means that two reasons account for anode erosion. First, the joule heat generated by the anode arc root melts and evaporates the anode material. Second, erosion abrasion is created by the rapid and hot plasma discharge channel.

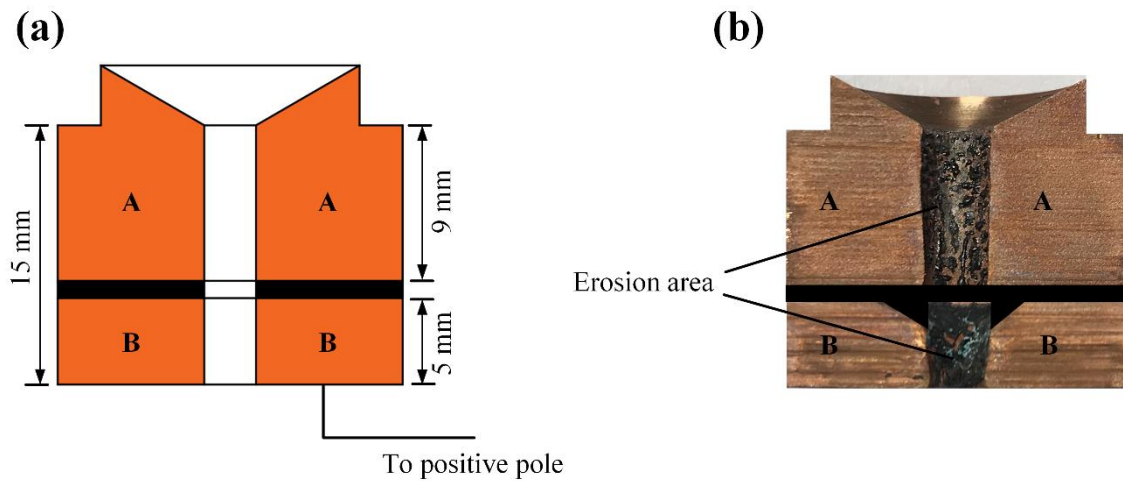


Fig. 12 Schematic of divided anode and the result

3.5 Surface morphology of erosion area

Generally, anode erosion is regarded as a process in which the anode material melts and evaporates under high temperature or reacts with oxygen ions in plasma and produces metal oxide, resulting in anode material loss. The surface morphology of an eroded anode is investigated to reveal the mechanism of anode erosion.

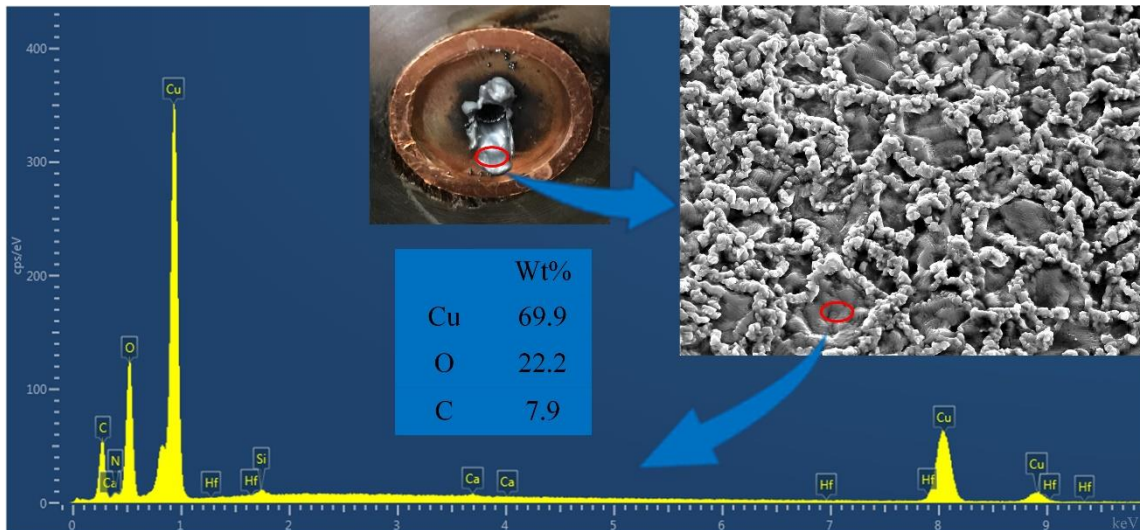


Fig. 13. Anode ablation products and EDS result

Fig. 13 shows the anode ablation products and the result of energy dispersive spectrometry (EDS). Most ablation products comprise copper oxide. The copper in the anode nozzle reacts with the high-temperature plasma and becomes copper oxide. The melted copper oxide is blown out of the nozzle. In the outlet of the anode nozzle, the melted copper oxide starts to solidify and clings to the anode as the temperature drops.

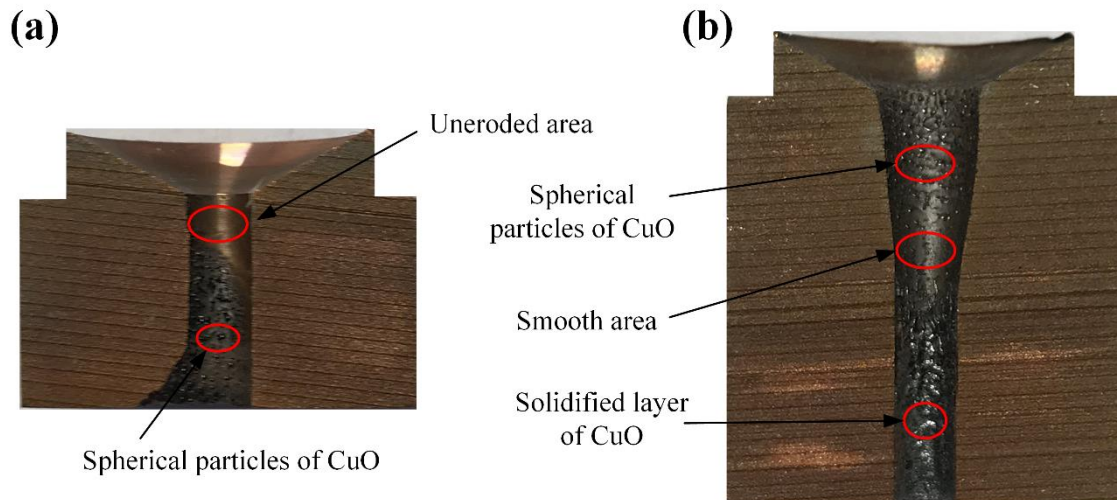


Fig. 14 Surface morphology of anode

Fig. 14 shows the surface morphology of the anode. The anode length shown in **Fig. 14(a)** is 10 mm, and it can be seen that in the inlet area, although this area is the nearest region to the cathode, there is no anode arc root in this area and no erosion trace is observed on the inside wall (the working time is short). The outlet of the anode is severely eroded, and the spherical particles of CuO cling to the inside wall of the anode. This outlet area is the discharge area. **Fig. 14(b)** shows the surface morphology of an anode measuring 20 mm in length. The spherical particles of CuO cling to the inlet area. A smooth corn-shaped area with no CuO particles on the surface is observed downstream. Gas velocity increases in this area because of the decrease in bore diameter. Melted CuO flows along the inner wall and forms a solidified layer in the further downstream area. This solidified layer covers the inner wall and protects the anode from erosion to some degree.

3.6 Anode erosion and its influence on plasma jet

Anode erosion reduces the lifetime of a plasma torch device and increases the instability of its performance. In several aspects, such as material synthesis, plasma coating, and plasma propulsion, the stability of the plasma torch is important, and the influence of anode erosion cannot be ignored. However, in other aspects, such as waste disposal and plasma drilling, the output power of the plasma torch plays an important role while instability is acceptable to some extent. Thus, the influence of anode erosion on plasma jet needs to be analyzed. **Fig. 15** shows the plasma jet when the anode length is 10 and 15 mm, respectively.

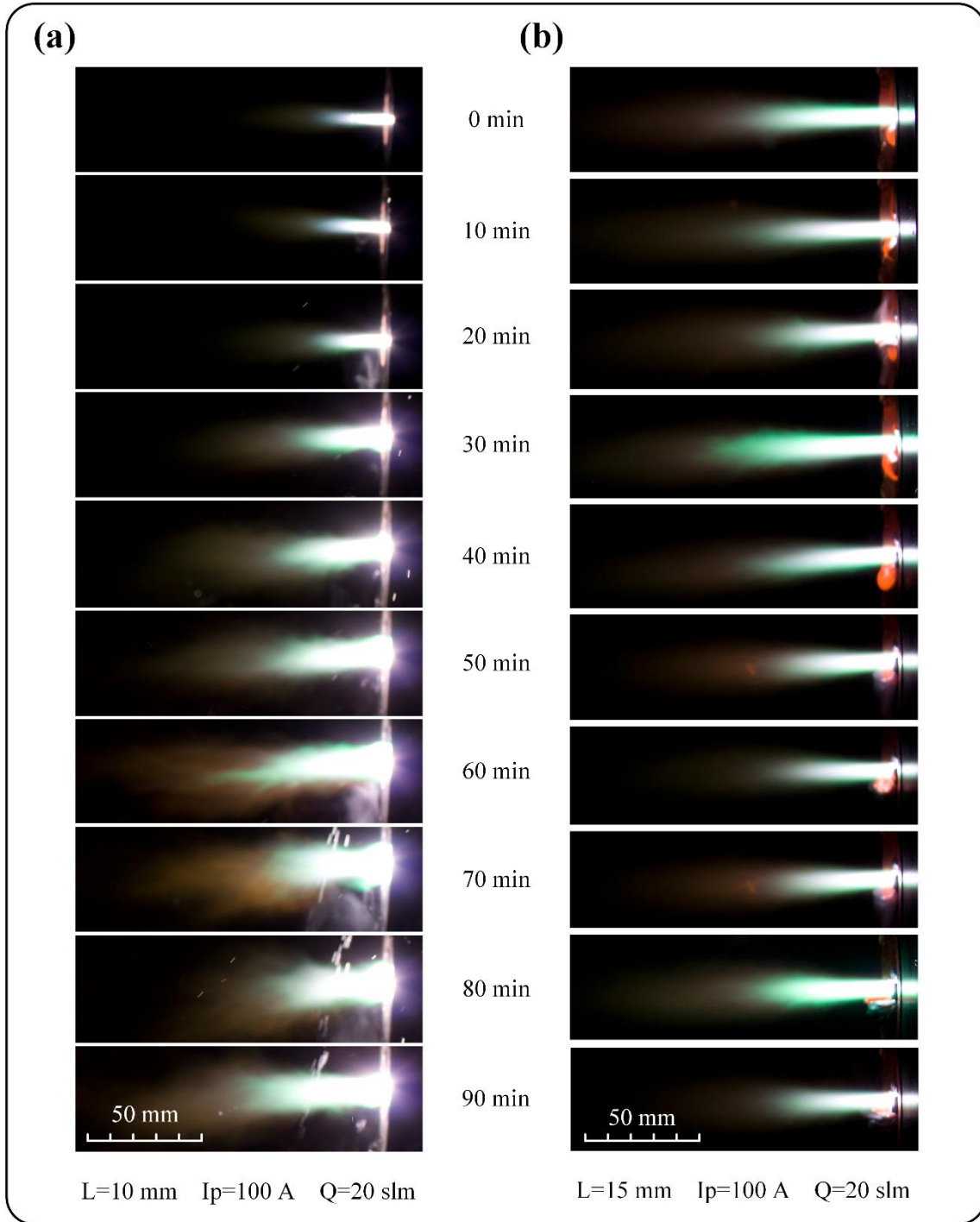


Fig. 15. Shape of plasma jet with changes in working time

The anode length in **Fig. 15(a)** is 10 mm. No erosion occurs on the anode, and the plasma jet is short and constricted in the beginning. The anode becomes horn shaped, and the plasma jet starts to be diffused and becomes unstable with the increase of working time. **Fig. 15(b)** shows the plasma jet when the anode length is 15 mm; in this situation, the cross section of eroded anode is cone shaped. Minimal change is observed in the shape of the plasma jet during the working time, and the discharge is stable. This result illustrates that erosion position plays an important role in the stability of plasma jets and that the shape of a plasma jet is related to the outlet of the anode nozzle. Erosion position moves from the outlet to the inlet with the increase of anode length. This condition can increase the stability of the plasma torch.

4. Conclusion

In this work, anode weight loss and anode erosion position with changes in plasma current, gas-flow rate, anode length, and plasma power were investigated. The relationship between anode erosion position and the position of the anode arc root and the power flow through the arc root was studied with divided anodes. The mechanism of anode erosion was studied, and the influence of anode erosion on plasma jet was investigated. The following conclusions were drawn.

1. Anode weight loss increases with changes in working time, and it increases with plasma current for Joule heat increases with the current. A large quantity of anode material can melt and evaporate in high current.

2. There is no significant difference in anode weight loss between the axial gas flow manner and tangential gas flow manner. Tangential gas flow has limited effect in making the erosion distribute evenly and cannot reduce anode weight loss.

3. The erosion extends along the former erosion area and the eroded area is more likely to be eroded again. Large plasma current will intensify this trend.

4. The anode weight loss decreases with the anode length and it is caused by the decrease of plasma power. With the increase of anode length, the anode erosion area moves from the outlet of the anode to the inlet.

5. With the increase of gas-flow rate, the energy flow through anode increases, and as a result, the anode weight loss increases. The erosion area moves from inlet to outlet of anode in this process. When anode arc root moves to the outlet of anode, there will be a jump in plasma power and anode weight loss. After that, with the continue increase of gas-flow rate, plasma power and anode erosion will not increase obviously anymore.

6. Divided anode method can be used to predict the anode shape after being eroded. Anode erosion position is mostly determined by the position of the anode arc root, and the erosion condition depends on the power flow through the arc root.

7. Erosion position plays an important role in the stability of plasma jets and the shape of a plasma jet is related to the outlet of the anode nozzle. Long anode nozzle can increase the stability of the plasma torch.

Data availability statement

The data that support the findings of this study are available from the corresponding author upon reasonable request.

Competing interests

The authors declare no competing financial interests.

Funding

The work is partially supported by a grant from Chinese National Natural Science Foundation (Grant No. 51774316).

Authors' contributions

Sun Qiang, Liu Yonghong and Han Yancong were in charge of the whole trial; Sun Qiang wrote the manuscript. All authors read and approved the final manuscript.

Acknowledgements

Not applicable.

Reference

¹ Chhowalla M and Unalan H E, "Thin films of hard cubic Zr₃N₄ stabilized by stress," *Nat. Mater.* **4**, 317 (2005)

² Tan Y Z, Chen R T, Liao Z J, Li J, Zhu F, Lu X, Xie S Y, Li J, Huang R B and Zhen L S, "Carbon arc

- production of heptagon-containing fullerene,” *Nat. Commun.* **2**, 420 (2011)
- ³ Huang H, Kajiura H, Tsutsui S, Hirano Y, Miyakoshi M, Yamada A and Ata M, “Large-scale rooted growth of aligned super bundles of single walled carbon nanotubes using a directed arc plasma method,” *Chem. Phys. Lett.* **343**, 7 (2001)
- ⁴ W X Pan, X Meng, H J Huang and C K Wu, “Effects of anode temperature on the arc volt-ampere characteristics and ejected plume property of a low-power supersonic plasma,” *Plasma Sources Sci. Technol.* **20**, 065006 (2011)
- ⁵ Haixing Wang, Weiping Sun, Surong Sun, A. B. Murphy and Yiguang Ju, “Two-Temperature chemical-nonequilibrium modelling of a high-velocity argon plasma flow in a low-power arcjet thruster,” *Plasma Chem. Plasma Process.* **43**, 559 (2014)
- ⁶ Tao Ma, Haixing Wang, Qi Shi, Shining Li and Anthony B Murphy, “Breakdown and current-voltage characteristics of DC micro-slit discharges in carbon dioxide,” *Plasma Sources Sci. Technol.* **27**, 075011 (2018)
- ⁷ I. R. Jankov, R. N. Szente, I. D. Goldman, M. N. P. Carreño, M. A. Valle, M. Behar, C. A. R. Costa, F. Galambeck and R. Landers, “Modification of electrode materials for plasma torches” *Surf. Coat. Technol.* **200**, 254 (2018)
- ⁸ R. N. Szente, R. J. Munz and M. G., “Drouet Arc velocity and cathode erosion rate in a magnetically driven arc burning in nitrogen,” *J. Phys. D-Appl. Phys.* **21**, 909 (1988)
- ⁹ Jin Myung Park Keun Su Kim, Tea Hyung Hwang and Sang Hee Hong, “Three-dimensional modeling of arc root rotation by external magnetic field in nontransferred thermal plasma torches,” *IEEE Trans. Plasma Sci.* **32**, 479 (2004)
- ¹⁰ Pavel Kotalko and Hideya Nishiyama, “An effect of magnetic field on arc plasma flow,” *IEEE Trans. Plasma Sci.* **30**, 160 (2002)
- ¹¹ X. Sun and J. Heberlein, “Fluid dynamic effects on plasma torch anode erosion,” *J. Therm. Spray Technol.* **14**, 39 (2005)
- ¹² Renzhong Huang, Hirotaka Fukanuma, Yoshihiko Uesugi, and Yasunori Tanaka, “An improved local thermal equilibrium model of DC arc plasma torch,” *IEEE Trans. Plasma Sci.* **39**, 1974 (2011)
- ¹³ Cheng Wang, Zelong Zhang, Weiluo Xia, Haichao Cui, and Weidong Xia, “Direct observation of anode arc root behaviors in a non-transferred arc plasma device with multiple cathodes,” *Plasma Chem. Plasma Process.* **37**, 371 (2017)
- ¹⁴ Cheng Wang, Lu Sun, Qiang Sun, Zelong Zhang, Weiluo Xia and Weidong Xia, “Experimental observation of constricted and diffuse anode attachment in a magnetically rotating arc at atmospheric pressure,” *Plasma Chem. Plasma Process.* **39**, 407 (2019)
- ¹⁵ Cheng Wang, Qiang Sun, Lu Sun, Zhongshan Lu, Weiluo Xia and Weidong Xia, “Spot and diffuse mode of cathode attachment in a magnetically rotating arc plasma generation at atmospheric pressure,” *J. Appl. Phys.* **125**, 033301 (2019)
- ¹⁶ Pan Wenxia, Li Teng, Meng Xian, Chen Xi, and Wu Chengkang, “Arc root attachment on the anode surface of arc plasma torch observed with a novel method,” *Chin. Phys. Lett.* **22**, 2895 (2005)
- ¹⁷ Pan Wenxia, Meng Xian, Li Teng, Chen Xi, and Wu Chengkang, “Comparative observation of Ar, Ar-H₂ and Ar-N₂ DC arc plasma jets and their arc root behaviour at reduced pressure,” *Plasma Sci. Technol.* **9**, 152 (2007)
- ¹⁸ Pan Wenxia, Chen Lewen, Meng Xian, Zhang Yong and Wu Chengkang, “Sufficiently diffused attachment of nitrogen arc by gasdynamic action,” *Theor. Appl. Mech. Lett.* **6**, 293 (2016)
- ¹⁹ Sun Qiang, Liu Yonghong, Han Yancong, Wu Xinlei, Liu Peng and Jin Hui, “A novel experimental method

of investigating anode-arc-root behaviors in a DC non-transferred arc plasma torch,” *Plasma Sources Sci. Technol.* **29**, 025008 (2020)